Available online at www.sciencedirect.com

ScienceDirect

Ceramics International 40 (2014) 101–107

CERAMICS INTERNATIONAL

www.elsevier.com/locate/ceramint

Enhanced photocatalytic performance of transition metal doped Bi_2O_3 nanoparticles under visible light irradiation

P. Malathy[a], K. Vignesh[b], M. Rajarajan[c,*], A. Suganthi[b,**]

[a]Department of Chemistry, N.M.S.S.V.N. College, Madurai 625019, Tamilnadu, India
[b]P.G. & Research Department of Chemistry, Thiagarajar College, Madurai 625009, Tamilnadu, India
[c]P.G. Department of Chemistry, Cardamom Planters' Association College, Bodinayakanur 626513, Tamilnadu, India

Received 30 April 2013; received in revised form 28 May 2013; accepted 28 May 2013
Available online 5 June 2013

Abstract

Transition metal (M=Ni and Zn) doped Bi_2O_3 nanoparticles were prepared by the precipitation method to enhance the photocatalytic activity of Bi_2O_3. The as-prepared nanoparticles were characterized by different techniques such as powder-X-ray diffraction (XRD), UV-vis diffuse reflectance spectroscopy (UV-vis-DRS), scanning electron microscopy (SEM), energy dispersive X-ray spectroscopy (EDX) and photoluminescence (PL) techniques. The photocatalytic activity was evaluated by the degradation of malachite green (MG) dye under visible light irradiation. The results revealed that Ni doped Bi_2O_3 (Ni-Bi_2O_3) exhibited higher photocatalytic activity when compared to that of other photocatalysts. A set of optimized conditions such as pH, catalyst concentration and initial dye concentration on the photodegradation of MG were investigated in detail.

Keywords: Bi_2O_3; Doping; Photodegradation; Visible light

1. Introduction

Our environment, which is endowed by nature, needs to be protected from ever increasing chemical pollution associated with contemporary life styles and emerging technologies. Developments in water treatment, have contributed to the improvement in our quality of life. Semiconductor photocatalysis has a great potential to contribute the environmental remediation especially in waste water treatment. TiO_2 and ZnO are ideal photocatalysts because of its chemical and biological inertness, stability against photocorrosion, non-toxicity, low cost [1–3]. However, their large band gap allows only a small portion of the solar spectrum (ultraviolet light region). Therefore, effective utilization of visible light (45% of solar spectrum) has become one of the most difficult challenges in photocatalysis [4–6].

Bi_2O_3 is an excellent visible light activated photocatalyst with a direct band gap of 2.8 eV [7]. The photocatalytic activity of Bi_2O_3 is further improved by doping with metal ions [8–11]. The photocatalytic activity of Zn modified Bi_2O_3 for the degradation of methyl orange, methylene blue and phenol were studied by Hameed et al. [12].The photocatalytic activity of Au–Bi_2O_3 nanorods was studied by Anandan et al. [13]. Xie et al. found that transition metal doped Bi_2O_3 (V^V, Pb^{II}, Ag^I and Co^{II}) showed higher photocatalytic activity than bare Bi_2O_3 under visible light [14].

MG is a kind of triphenyl methane dye which has been widely used in the production of ceramics, leather, textile industry, food coloring and cell coloring. Due to its high efficiency in disinfection, it has also been used in aquaculture industry to treat scratch on the fish bodies and defend against bacterial infections. The molecular structure of MG is shown in Fig. 1. Reduced forms of MG are highly toxic, persistent, carcinogenic and mutagenic. MG exposure results in a blockade of the hormone system, decreases T4 and increases FSH concentrations and causes thyroid tumors (or) forming DNA-adducts which causes liver and thyroid tumors [15]. The risks for human health include direct exposure for the workers in the dye manufacturing, textile and agriculture industries, indirect exposure from damage by waste water environment and consumption of the treated fish.

*Corresponding author. Fax: +91 4546 280793.
**Corresponding author. Fax: 91 452 2312375.
E-mail addresses: rajarajan_1962@yahoo.com (M. Rajarajan), suganthitcarts@gmail.com, suganthiphd09@gmail.com (A. Suganthi).

0272-8842/$ - see front matter © 2013 Elsevier Ltd and Techna Group S.r.l. All rights reserved.
http://dx.doi.org/10.1016/j.ceramint.2013.05.109

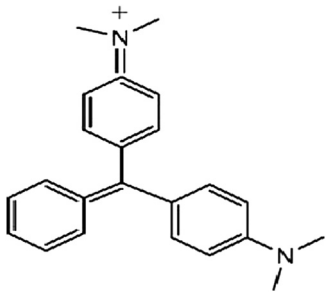

Fig. 1. Molecular Structure of MG.

Sayikan et al. [16] have studied the degradation of MG using Sn^{4+} doped TiO_2. Use of Fe^{3+} doped TiO_2 in photocatalytic bleaching of MG has been reported by Asilturk et al. [17]. Kaneva et al. [18] have examined the photocatalytic activity of Ni doped ZnO for the treatment of MG. Recently Zhang et al. [19] have investigated the photochemical decomposition of MG using $La_{1-x}Ba_xCoO_3$ nanopowders. These results prompted us to study the photocatalytic behavior of transition metal doped Bi_2O_3 towards the degradation of MG under visible light irradiation. The influences of operational parameters such as pH, catalyst concentration and initial dye concentration which affect the photocatalytic process have been investigated in detail.

2. Experimental

2.1. Materials

AR grade of Bismuth (III) nitrate, sodium hydroxide, sodium sulfate, nickel sulfate, zinc sulfate, ethanol and malachite green were purchased from Merck and applied without further purification. All solutions were prepared with double distilled water.

2.2. Catalyst preparation

Metal doped Bi_2O_3 (M-Bi_2O_3) was prepared by the following procedure (the molar ratio of Bi: metal is fixed at 1:0.25): 0.002 moles (0.25 M of 50 mL) of metal sulfate, 0.01 moles (1 M of 50 mL) of bismuth nitrate and 0.07 moles (1.5 M of 50 mL) of sodium sulfate were mixed and the solution was stirred at room temperature for 45 min. Then, 0.09 moles (0.9 M of 100 mL) of sodium hydroxide was added drop by drop into the above mixture with constant stirring until the completion of precipitation. The precipitate obtained was filtered, washed with double distilled water and ethanol. The samples were dried at 110 °C for 2 h followed by calcination at 500 °C for 3 h in a muffle furnace. Bi_2O_3 was also prepared by the same procedure without the addition of metal sulfate.

2.3. Characterization

The crystallite size of the catalyst was examined by X-ray diffractometer (XPERT PRO) with Cu Kα radiation. The surface morphology was characterized by SEM (JSM 6701F—6701) in both secondary and back scattered electron modes. The metal composition was investigated by an energy dispersive X-ray spectroscopy attached to the SEM. The optical property was determined by UV-vis diffuse reflectance spectroscopy (JASCO V-550) with PMT detector. Photoluminesence was recorded on fluorescence spectrometer (Perkin-Elmer LS 55). The photocatalytic experiments were performed in an immersion type photoreactor (HIPR-p-8/125/250/400) and pH was adjusted using a pH meter (EUTECH).

2.4. Photocatalytic experiments

The photocatalytic experiments were carried out in an immersion type photoreactor. The experimental procedure for the photodegradation of MG was similar to our previous reports [20,21]. 200 mL of aqueous solution with 5 μM concentration of MG was taken in a cylindrical glass vessel, in which air was bubbling continuously from the bottom of the reactor. Then, pH of the solution was adjusted using 0.1 N H_2SO_4 (or) 0.1 N NaOH and required amount of photocatalyst (0.25 gL^{-1}) was added into the vessel. Before irradiation, the reaction mixture was stirred in dark for 30 min to achieve the adsorption–desorption equilibrium between the catalyst and dye molecules. A 300 W Xe arc lamp with an ultra violet ($\lambda > 400$ nm) cut off filter was used as the visible light irradiation source. During the course of light irradiation, 5 mL aliquot was withdrawn at a regular time interval of 30 min. Then the samples were centrifuged and filtered through a millipore filter to remove the photocatalyst. The filtrate was analyzed by UV–visible spectrophotometer at λ_{max}=618 nm to evaluate the residual MG concentration.

$$\text{Photodegradation (\%)} = \frac{C_0 - C}{C_0} \times 100 \quad (1)$$

where C_0 is the concentration of MG before irradiation (t=0) and C is the concentration of MG after a certain irradiation time.

3. Results and discussion

3.1. XRD

The XRD patterns are presented in Fig. 2. The crystal structure of Bi_2O_3 is not affected but the peak intensities are changed, after doping with transition metal ions. All diffraction peaks are perfectly indexed with the tetragonal phase of Bi_2O_3 (JCPDS 65-1209). Also, the diffraction peaks due to transition metals (Ni and Zn) are not appeared. This may be due to their low content and extremely high dispersion.

The average crystallite size was estimated by Scherrer equation. $D = 0.89\lambda/\beta \cos\theta$, where λ = wavelength of X-rays, β = peak width of half maximum and θ = Bragg diffraction angle. The average crystallite sizes of Bi_2O_3, Ni-Bi_2O_3 and Zn-Bi_2O_3 were determined as 17 nm, 23 nm and 20 nm respectively.

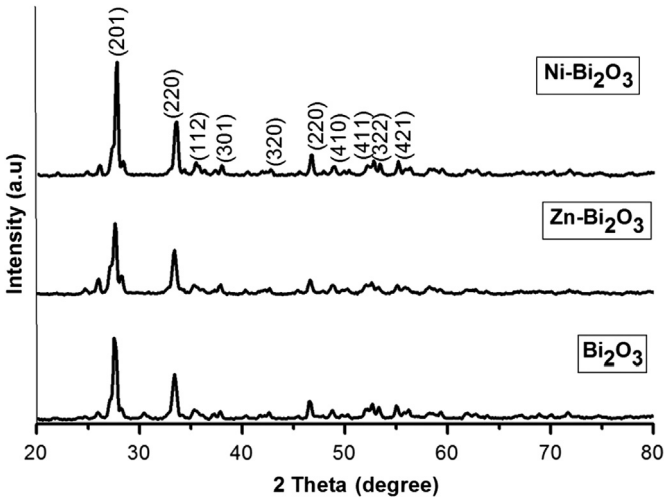

Fig. 2. XRD patterns of Bi_2O_3, Ni-Bi_2O_3 and Zn-Bi_2O_3.

3.2. SEM and EDX

The morphology of Bi_2O_3 and M-Bi_2O_3 were analyzed by SEM. The results are shown in Fig. 3. Bi_2O_3 and Ni-Bi_2O_3 have rod like structures and flower like structures are observed for Zn-Bi_2O_3. These morphological changes are induced by the addition of transition metals.

Fig. 4 shows the EDX spectra of Bi_2O_3 and M-Bi_2O_3 samples. The EDX data of all samples are listed in the Table 1. The Bi content decreases after doping with transition metal cations.

3.3. UV–vis-DRS

Fig. 5. shows the UV–vis-DRS of Bi_2O_3, Ni-Bi_2O_3 and Zn-Bi_2O_3. As seen from the figure, the presence of Ni ions in Bi_2O_3 showed significant absorption shift into the visible region compared to Bi_2O_3. A plot of $(\alpha h\nu)^{1/2}$ versus $h\nu$ afforded band gap of all samples. Fig. 6 exhibits the Tauc plots of Bi_2O_3, Ni-Bi_2O_3 and Zn-Bi_2O_3. The band gaps of Bi_2O_3, Ni-Bi_2O_3 and Zn-Bi_2O_3 were found to be 2.8 eV, 2.69 eV and 2.74 eV respectively. The narrow band gap of Ni-Bi_2O_3 depicted that it should possesses excellent visible light photocatalytic activity than that of Zn-Bi_2O_3 and Bi_2O_3.

3.4. Photoluminesence (PL) spectra

The efficiency of photocatalytic activity and charge trapping in the semiconductor could be verified by PL spectra [22]. Fig. 7 shows the PL spectrum of Bi_2O_3, Ni-Bi_2O_3 and Zn-Bi_2O_3 nanoparticles. The intensity of the luminescence peak of Ni-Bi_2O_3 is much weaker than that of Bi_2O_3. The luminescence of semiconductor is mainly caused by the recombination of photoinduced electrons and holes [23]. Therefore, the doping of Ni could effectively separate photoinduced electrons from holes on the surface of Bi_2O_3, thus inhibiting their recombination, resulting in enhanced photocatalytic activity [14].

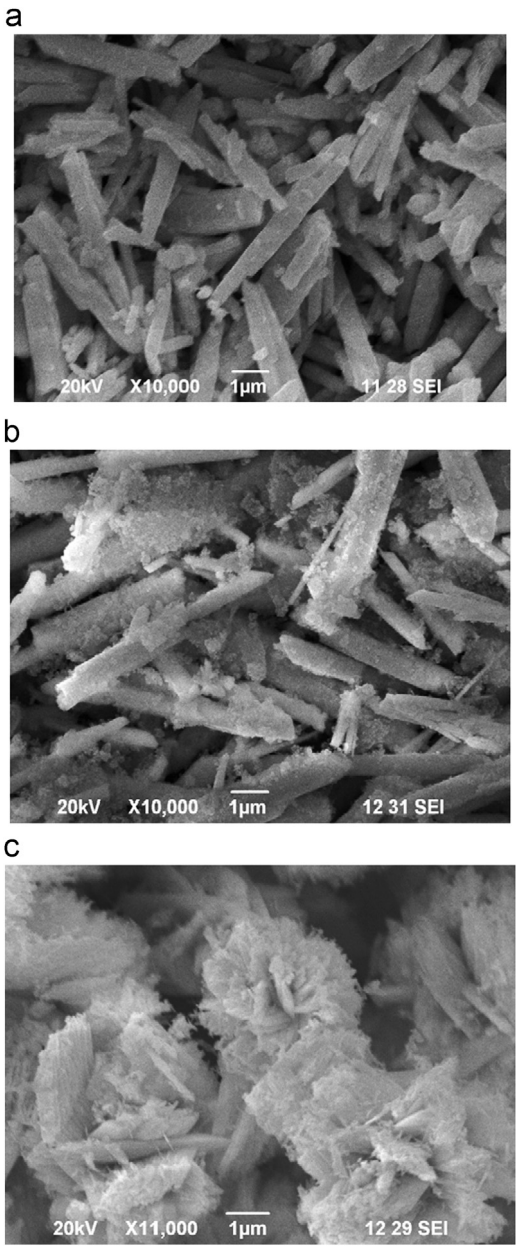

Fig. 3. SEM images of (a) Bi_2O_3 (b) Ni-Bi_2O_3 and (c) Zn-Bi_2O_3.

4. Photodegradation of MG

The photocatalytic activity of Bi_2O_3 (0.25 g L^{-1}) and M-Bi_2O_3 (0.25 g L^{-1}) was investigated by measuring the degradation of MG (5 μM) in aqueous solution at pH 5. Fig. 8 depicts the photodegradation efficiency of Bi_2O_3, Ni-Bi_2O_3 and Zn-Bi_2O_3. The photocatalytic activity of Ni-Bi_2O_3 is obviously higher than that of Bi_2O_3 (24%) and Zn-Bi_2O_3 (27%). It is deduced that, doping of Ni into Bi_2O_3 can introduce new electronic states in Bi_2O_3 to form a additional interband site [13,24,25]. The electron trapping by this interband site lead to the suppression of electron–hole recombination process and therefore efficient electron-hole separation is achieved on the photocatalyst surface. Therefore, Ni doping increases the number of photogenerated electrons and

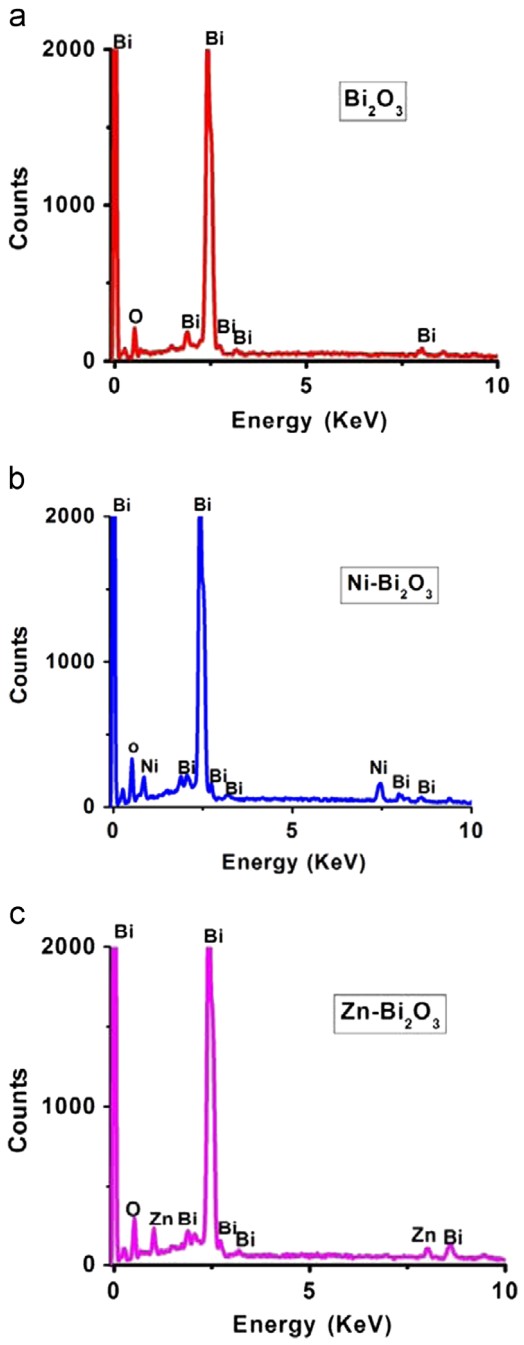

Fig. 4. EDX spectra of Bi_2O_3, Ni-Bi_2O_3 and Zn-Bi_2O_3.

Table 1
EDX data of Bi_2O_3, Ni-Bi_2O_3 and Zn-Bi_2O_3.

Element	Bi_2O_3		Ni-Bi_2O_3		Zn-Bi_2O_3	
	Weight %	Atomic %	Weight %	Atomic %	Weight %	Atomic %
Bi	86.81	33.5	77.42	24.71	76.65	24.67
O	13.19	66.5	16.36	68.23	16.51	67.84
Transition metal	–	–	6.22	7.06	6.84	7.49
Gross	100		100	100	100	100

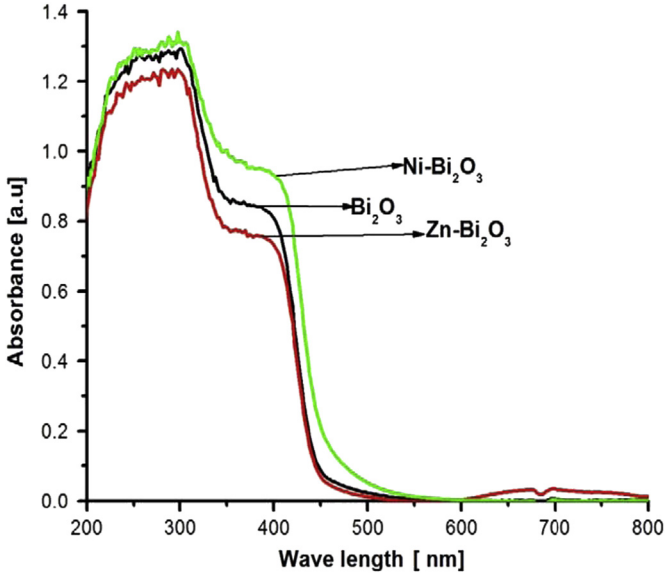

Fig. 5. UV–vis-DRS of Bi_2O_3, Ni-Bi_2O_3 and Zn-Bi_2O_3.

holes to participate in the photocatalytic reaction, which results in high photocatalytic activity.

According to the previously published literatures [26,27]. We have proposed a mechanism for the enhanced photocatalytic activity of Ni-Bi_2O_3. It can be described as follows:

$$Bi_2O_3 + h\nu \rightarrow h^+_{VB} + e^-_{CB} \quad (2)$$

$$Ni^{2+} + h^+ \rightarrow Ni^{3+}(\text{hole trap}) \quad (3)$$

$$Ni^{2+} + e^- \rightarrow Ni^{+}(\text{electron trap}) \quad (4)$$

When Bi_2O_3 is irradiated by visible light, holes (h^+_{VB}) and electrons (e^-_{CB}) are generated in its valence band and conduction band respectively. The photogenerated electrons and holes combine with Ni $^{2+}$ ions to form Ni^{3+} and Ni^{+} ions respectively.

$$Ni^{+} + O_2 \rightarrow Ni^{2+} + O_2^{\bullet -} \text{ (electron release)} \quad (5)$$

$$Ni^{3+} + OH^- \rightarrow Ni^{2+} + O\ H \text{ (hole .25}\textit{trueem}\text{ release)} \quad (6)$$

These super oxide anion ($O_2^{\bullet -}$) and hydroxyl radicals ($^{\bullet}OH$) are powerful oxidizing species and it will degrade MG.

4.1. Effect of pH

The degradation of MG was studied at different pH values (in the pH range of 3–9) with an initial MG concentration of 5 μM, catalyst concentration (Ni-Bi_2O_3) of 0.25 g L^{-1} and irradiation time of 180 min. The degradation of MG as a function of pH is shown in Fig. 9. The photodegradation of MG increases with increase in pH from 3 to 5 and a further increase in pH leads to a decrease in photodegradation. The photocatalytic activity of Ni-Bi_2O_3 was found to be 88% at pH 5. MG degradation profile over Ni-Bi_2O_3 as a function of irradiation time is presented in Fig. 12.

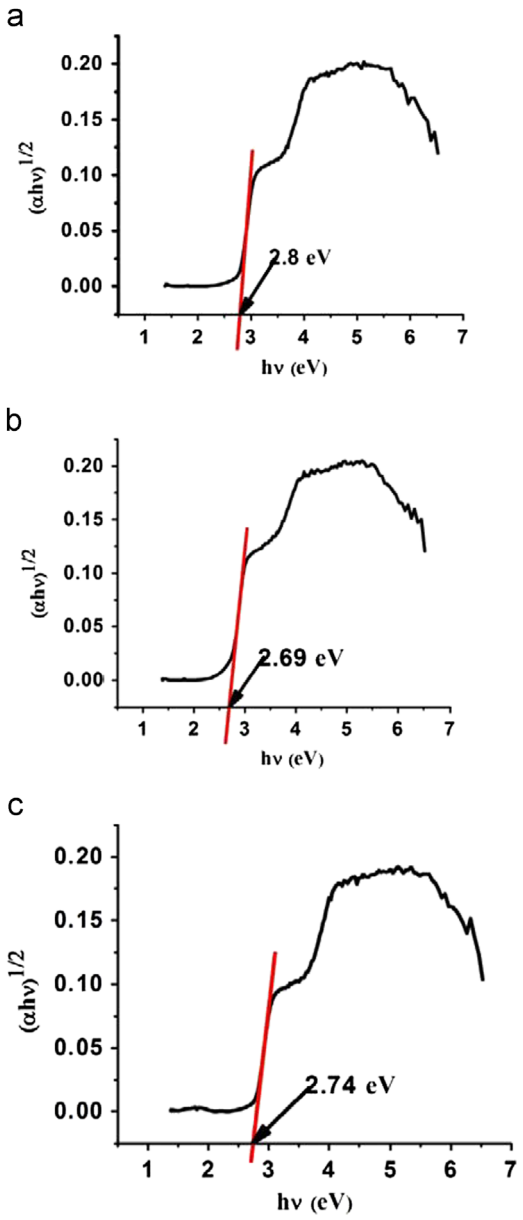

Fig. 6. Tauc plots of (a) Bi_2O_3 (b) Ni-Bi_2O_3 and (c) Zn-Bi_2O_3.

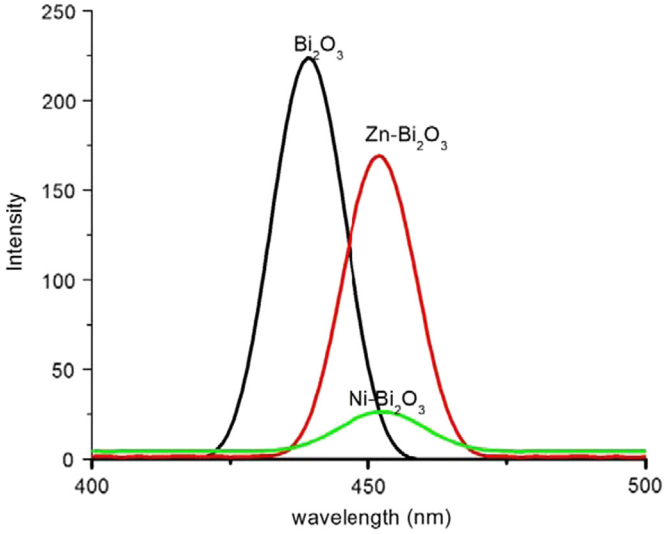

Fig. 7. PL Spectra of Bi_2O_3, Ni-Bi_2O_3 and Zn-Bi_2O_3.

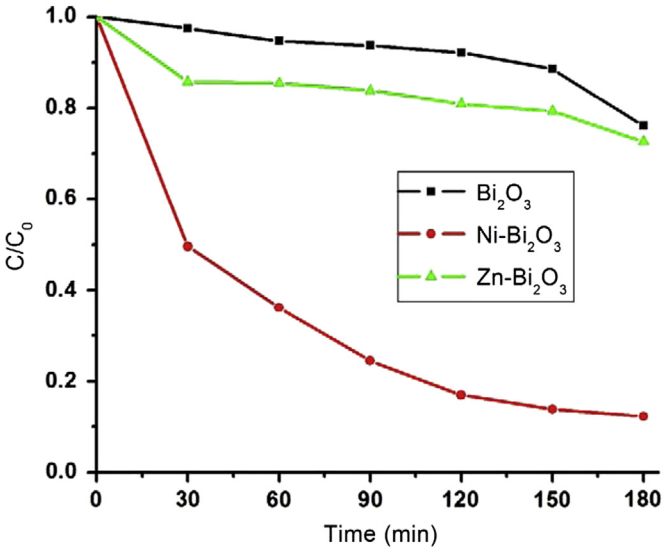

Fig. 8. Effect of catalyst (Bi_2O_3, Ni-Bi_2O_3 and Zn-Bi_2O_3) on the degradation of MG at pH 5.

4.2. Effect of concentration of the catalyst

MG degradation is also influenced by various concentrations of Ni-Bi_2O_3 from 0.125 g L^{-1} to 0.375 g L^{-1} and the other reaction parameters were kept constant [MG concentration = 5 μM, pH = 5 and irradiation time = 180 min] and the results are compiled in Fig. 10. The photodegradation of MG increases with increase in photocatalyst concentration from 0.125 g L^{-1} to 0.25 g L^{-1} and a further increase in catalyst concentration leads to decrease in photodegradation. The observed results revealed that the increase in catalyst concentration, increases the number of active sites on Ni-Bi_2O_3 surface thus increases in the number of $^{\bullet}OH$ radicals which can take part in the degradation of MG. Beyond 0.25 g L^{-1} of Ni-Bi_2O_3, the solution becomes turbid and thus blocks visible light for the reaction to proceed and therefore photodegradation starts decreasing. Hence, the optimum catalyst concentration of Ni-Bi_2O_3 was found to be 0.25 g L^{-1}.

4.3. Effect of the initial MG concentration

The influence of initial MG concentration on its photodegradation was examined in the presence of Ni-Bi_2O_3 (0.25 g L^{-1}) at pH 5 is displayed in Figs. 11 and 12. The photodegradation of MG decreases with increase of MG concentration from 5 μM to 7 μM. At high MG concentrations, more MG molecules are adsorbed on the surface of Ni-Bi_2O_3, and less number of photons is available to reach the catalyst surface and therefore less number of $^{\bullet}OH$ is formed, thus causing an inhibition in degradation percentage. Also, the increase MG concentration can be lead to decrease the path

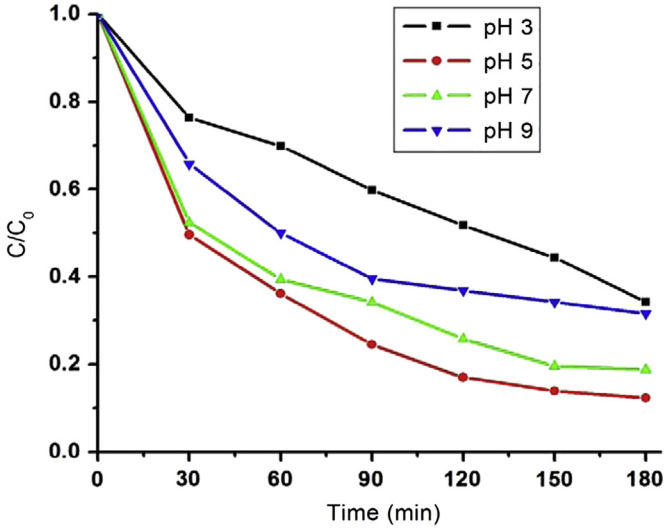

Fig. 9. Effect of pH on the degradation of MG (Ni-Bi_2O_3).

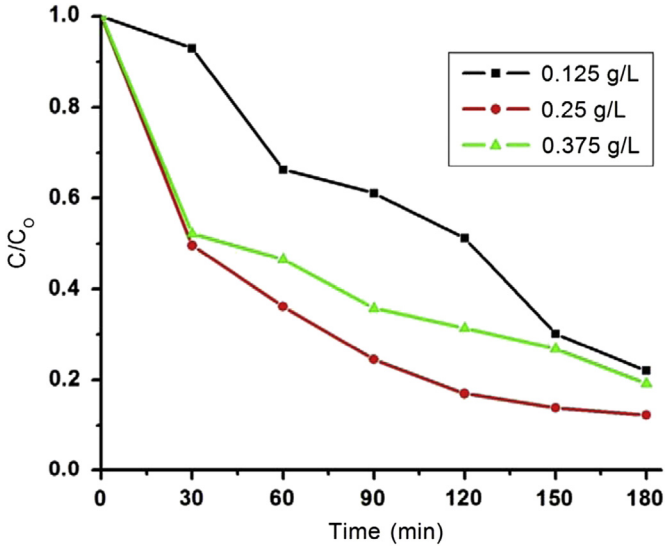

Fig. 10. Effect of catalyst concentration (Ni-Bi_2O_3) on the degradation of MG at pH 5.

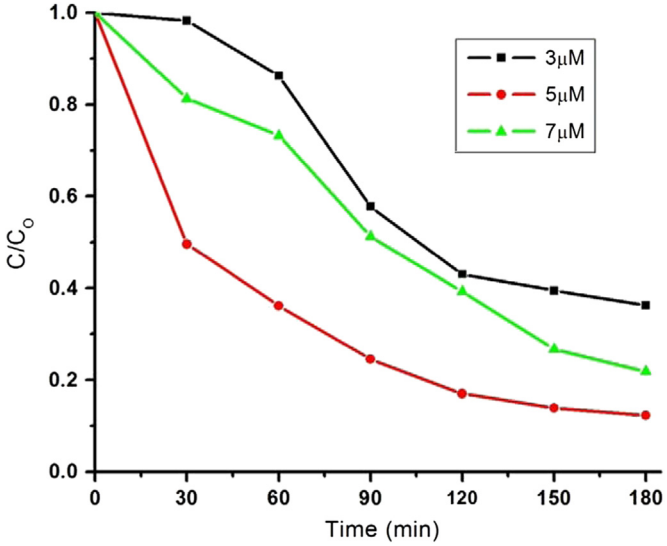

Fig. 11. Effect of Concentration of MG and its photodegradation.

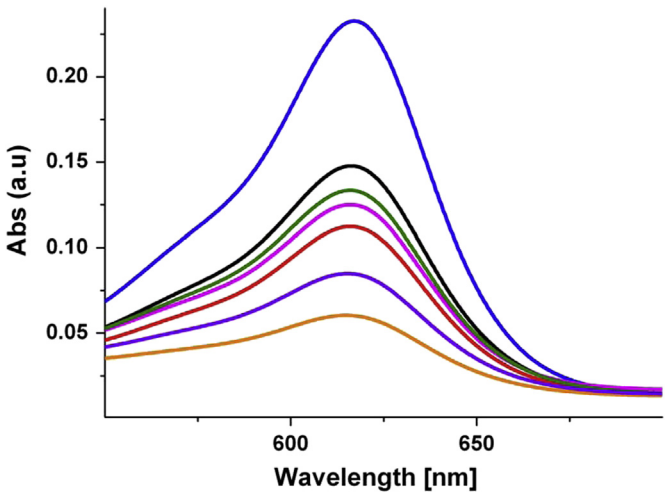

Fig. 12. Absorption changes of MG Photodegradation using Ni-Bi_2O_3.

length of photon entering the aqueous solution of MG and reduce the catalytic efficiency [28].

5. Conclusion

In this study, photodegradation of MG has been investigated using both Bi_2O_3 and M-Bi_2O_3. This study shows that the photocatalytic activity of Ni-Bi_2O_3 is maximum due to significant absorption shift into the visible region. XRD results showed that there were no changes in the structure of the catalyst as a result of doping with the metal ions. So, doping imparted distinct morphological and light absorption differences. PL spectra showed that the doping of Ni, inhibit the recombination of the electron and hole pairs on the surface of Bi_2O_3. The maximum percentage of MG photodegradation was achieved with Ni-Bi_2O_3 concentration of 0.25 g L^{-1}, initial MG concentration of 5 μM, pH 5 and irradiation time of 180 min. Ni-Bi_2O_3 may be used as an efficient photocatalyst for the degradation of organic pollutants under visible light.

Acknowledgment

The authors are also thankful to the Managements of N.M.S. S.V.N. College, Thiagarajar College and Cardamom Planter's Association College for providing the necessary laboratory facilities.

References

[1] A. Fujishima, T.N. Rao, D.A. Tryk, Titaniumdioxide photocatalysis, Journal of Photochemistry and Photobiology C: Photochemistry Reviews 1 (2000) 1–21.

[2] Y. Liu, F. Xin, F. Wang, S. Luo, X. Yin, Synthesis and characterization and activities of visible light –driven Bi_2O_3–TiO_2 composite photocatalysts, Journal of Alloys and Compounds 498 (2010) 179–184.

[3] E.J. Li, K. Xia, S.F. Yin, W.L. Dai, S.L. Luo, C.T. Au, Preparation, characterization and photocatalytic activity of Bi_2O_3–MgO, Materials Chemistry and Physics 125 (2011) 236–241.
[4] V. Stengl, S. Bakardjieva, N. Murafa, Preparation and Photocatalytic activity of rare earth doped TiO_2 nanoparticles, Materials Chemistry and Physics 114 (2009) 217–226.
[5] D. Jung, Syntheses and characterization of transition metal-doped ZnO, Solid State Sciences 12 (2010) 466–470.
[6] J.X. Sun, G. Chen, Y.X. Li, C. Zhon, H.J. Zhang, A novel photocatalyst and improvement of photocatalytic properties by Cu doping, Journal of Alloys and Compounds 509 (2011) 1113–1137.
[7] H. Abdul, M. Tiziano, G. Valentina, P. Fornasiero, Surface phases and photocatalytic activity correlation of Bi_2O_3/Bi_2O_{4-x} nanocomposite, Journal of the American Chemical Society 130 (2008) 9658–9689.
[8] L. Li, B. Yan, CeO_2–Bi_2O_3 nanocomposite: two step synthesis, microstructure and photocatalytic activity, Journal of Non-Crystalline Solids 355 (2009) 776–779.
[9] L. Li, B. Yan, $BiVO_4/Bi_2O_3$ submicrometer sphere composite: microstructure and photocatalytic activity under visible-light irradiation, Journal of Alloys and Compounds 476 (2009) 624–628.
[10] L. Jing, J. Wang, Y. Qu, Y. Luan, Effects of surface-modification with Bi_2O_3 on the thermal stability and photo induced charge property of nanocrystalline anatase TiO_2 and its enhanced photocatalytic activity, Applied Surface Science 256 (2009) 657–663.
[11] T. Saison, N. Chemin, C. Chaneac, O. Durupthy, V. Ruaux, L. Mariey, F. Mauge, P. Beaunier, J.P. Jolivet, Bi_2O_3, $BiVO_4$ and Bi_2WO_6: impact of surface properties on photocatalytic activity under sunlight, Journal of Physical Chemistry C, 115, 5657–5666.
[12] A. Hameed, V. Gombac, T. Montini, L. Felisari, P. Fornasiero, Photocatalytic activity of zinc modified Bi_2O_3, Chemical Physics Letters 483 (2009) 254–261.
[13] S. Anandan, G. Lee, P. Chen, C. Fan, J. Wu, Removal of orange II dye in water by visible light assisted photocatalytic ozonation using $Bi_2O_3$and Au/Bi_2O_3 nanorods, Industrial and Engineering Chemistry Research 49 (2010) 9729–9737.
[14] J. Xie, X. Lu, M. Chen, G. Zhao, Y. Song, S. Lu, The synthesis, characterization and photocatalytic activity of V(V), Pb(II), Ag(I) and Co (II)-doped Bi_2O_3, Dyes and Pigments 77 (2008) 43–47.
[15] A. Bojinova, C. Dushkin, Photodegradation of malachite green in water solutions by means of thin films of TiO_2/WO_3 under visible light, Reaction Kinetics, Mechanisms and Catalysis 103 (2011) 239–250.
[16] F. Sayikan, M. Asilturk, P. Tatar, N. Kiraz, E. Arpac, H. Sayikan, Photocatalytic performance of Sn-doped TiO_2 nanostructured thin films for photocatalytic degradation of malachite green dye under UV–vis-lights, Materials Research Bulletin 43 (2008) 127–134.
[17] M. Asilturk, F. Sayilkan, E. Arpac, Effect of Fe^{3+} ion doping to TiO_2 on the photocatalytic degradation of malachite green dye under UVand VIS-irradation, Journal of Photochemistry and Photobiology A: Chemistry 203 (2009) 64–71.
[18] N.V. Kaneva, D.T. Dimitrov, C.D. Dushkin, Effect of nickel doping on the photocatalytic activity of ZnO thin films under UV and visible light, Applied Surface Science 257 (2011) 8113–8120.
[19] C. Zhang, H. He, N. Wang, H. Chen, D. Kong, Visible-light sensitive $La_{1-x}Ba_xCoO_3$ photocatalyst for malachite green degradation, Ceramics International 39 (2013) 3685–3689.
[20] K. Vignesh, A. Suganthi, M. Rajarajan, R. Sakthivadivel, Visible light assisted photodecolourization of eosin-Y in aqueous solution using hesperidin modified TiO_2 nanoparticles, Applied Surface Science 258 (2012) 4592–4600.
[21] K. Vignesh, A. Suganthi, M. Rajarajan, S.A. Sara, Photocatalytic activity of AgI sensitized ZnO nanoparticles under visible light irradiation, Powder Technology 224 (2012) 331–337.
[22] J.G. Yu, H.G. Yu, B. Cheng, X.J. Zhao, J.C. Yu, W.K. Ho, The effect of calcinations temperature on the surface microstructure and photocatalytic activity of TiO_2 thin films prepared by liquid phase deposition, Journal of Physical Chemistry B 107 (2003) 13871–13879.
[23] W. Li, Preparation of monodisperse nanometer Bi_2O_3 powder, Journal of Central South University of Technology 36 (2005) 175–178.
[24] K.R. Jakkidi, S. Basavaraju, D.K. Valluri, Sm^{3+} doped Bi_2O_3 photocatalyst prepared by hydrothermal method, ChemCatChem 14 (2009) 492–496.
[25] J.B. Zhong, J.Z. Li, X.Y. He, J. Zeng, Y. Lu, E. Hu, K. Lin, Improved photocatalytic performance of Pd-doped ZnO, Current Applied Physics 12 (2012) 998–1001.
[26] L.G. Devi, S.G. Kumar, Influence of physicochemical-electronic properties of transition metal ion doped polycrystalline titania on the photocatalytic degradation of Indigo carmine and 4-nitrophenol under UV/solar light, Applied Surface Science 257 (2011) 2779–2790.
[27] B. Pare, B. Sarwan, S.B. Jonnlagadda, Photocatalytic mineralization study of malachite green on the surface of Mn-doped BiOCl activated by visible light under ambient condition, Applied Surface Science 258 (2011) 247–253.
[28] I. Poulios, A. Avranas, E. Rekliti, A. Zouboulis, Photocatalytic oxidation of Auramine O in the presence of semiconducting oxides, Journal of Chemical Technology and Biotechnology 75 (2000) 205–212.